Journal of Neurochemistry
Lippincott Williams & Wilkins, Inc., Philadelphia

Characterization of Copper Interactions with Alzheimer Amyloid β Peptides: Identification of an Attomolar-Affinity Copper Binding Site on Amyloid β1–42

*†‡Craig S. Atwood, *†‡Richard C. Scarpa, *†‡Xudong Huang, ‡§Robert D. Moir, *†‡Walton D. Jones, ‖David P. Fairlie, ‡§Rudolph E. Tanzi, and *†‡Ashley I. Bush

**Laboratory for Oxidation Biology, Departments of †Psychiatry and §Neurology, and ‡Genetics and Aging Unit, Massachusetts General Hospital and Harvard Medical School, Boston, Massachusetts, U.S.A.; and ‖Centre for Drug Design and Development, University of Queensland, Brisbane, Queensland, Australia*

Abstract: Cu and Zn have been shown to accumulate in the brains of Alzheimer's disease patients. We have previously reported that Cu^{2+} and Zn^{2+} bind amyloid β (Aβ), explaining their enrichment in plaque pathology. Here we detail the stoichiometries and binding affinities of multiple cooperative Cu^{2+}-binding sites on synthetic Aβ1–40 and Aβ1–42. We have developed a ligand displacement technique (competitive metal capture analysis) that uses metal–chelator complexes to evaluate metal ion binding to Aβ, a notoriously self-aggregating peptide. This analysis indicated that there is a very-high-affinity Cu^{2+}-binding site on Aβ1–42 (log K_{app} = 17.2) that mediates peptide precipitation and that the tendency of this peptide to self-aggregate in aqueous solutions is due to the presence of trace Cu^{2+} contamination (customarily ~0.1 μ*M*). In contrast, Aβ1–40 has much lower affinity for Cu^{2+} at this site (estimated log K_{app} = 10.3), explaining why this peptide is less self-aggregating. The greater Cu^{2+}-binding affinity of Aβ1–42 compared with Aβ1–40 is associated with significantly diminished negative cooperativity. The role of trace metal contamination in inducing Aβ precipitation was confirmed by the demonstration that Aβ peptide (10 μ*M*) remained soluble for 5 days only in the presence of high-affinity Cu^{2+}-selective chelators. **Key Words:** Human amyloid β peptide—Copper—Affinity—Stoichiometry—Alzheimer's disease—Binding affinity method—Chelators.
J. Neurochem. **75,** 1219–1233 (2000).

Alzheimer's disease (AD) is characterized pathologically by the deposition of amyloid plaques and neurofibrillary tangles and by neuronal degeneration in the brains of affected individuals. Amyloid deposits are composed primarily of the amyloid β (Aβ) protein (Masters et al., 1985; Roher et al., 1996) generated as a mixture of polypeptides manifesting carboxyl- and amino-terminal heterogeneity. The Aβ1–40 isoform is the predominant soluble species in biological fluids (Shoji et al., 1992; Vigo-Pelfrey et al., 1993). Although less abundant in biological fluids, Aβ1–42 is the predominant species found in plaque deposits (Masters et al., 1985; Roher et al., 1996).

Metal ion homeostasis is severely dysregulated in AD (Hershey et al., 1983; Ehmann et al., 1986; Thompson et al., 1988; Vance et al., 1990; Basun et al., 1991; Samudralwar et al., 1995; Deibel et al., 1996; Cornett et al., 1998; Lovell et al., 1998; González et al., 1999). Although the transition metal ions Cu, Fe, and Zn are maintained at high concentrations within the healthy brain neocortical parenchyma (total dry weight concentrations of 70, 340, and 350 μ*M*, respectively), increased concentrations of these metal ions are detected in the neuropil of the AD-affected brain, where they are highly concentrated within amyloid plaque deposits with total concentrations reaching ~0.4 and ~1 m*M* for Cu and Fe/Zn, respectively (Lovell et al., 1998). An elevated Zn^{2+} concentration also can be detected in plaque deposits histologically (Suh et al., 2000). We previously found that Aβ avidly binds Cu^{2+}, Zn^{2+}, and Fe^{3+} (Bush et al., 1994*a*,*b*, 1995; Huang et al., 1997; Atwood et al., 1998), perhaps explaining the recruitment of these metals into amyloid plaque pathology.

Evidence for an interaction between Cu^{2+} and Aβ1–40 was first observed by the stabilization of an

Resubmitted manuscript received April 4, 2000; accepted April 18, 2000.

Address correspondence and reprint requests to Dr. A. I. Bush at Laboratory for Oxidation Biology, Genetics and Aging Unit, Neuroscience Center, Massachusetts General Hospital East, Building 149, 13th Street, Charlestown, MA 02129-9142, U.S.A. E-mail: bush@helix.mgh.harvard.edu

Drs. C. S. Atwood and R. C. Scarpa contributed equally to this article.

Abbreviations used: Aβ, amyloid β; AD, Alzheimer's disease; CDTA, *trans*-1,2-diaminocyclohexane-*N*,*N*,*N*′,*N*′-tetraacetic acid; CMCA, competitive metal capture analysis; DSA, dog serum albumin; DTPA, diethylenetriaminepentaacetic acid; PAGE, polyacrylamide gel electrophoresis; SDS, sodium dodecyl sulfate.

Exhibit 9

FIG. 1. Simplified principle of CMCA. Known amounts of protein, chelator, and metal ion are brought into equilibrium. An array of chelators of known log K_{app1} is presented to this equilibrium system, and the perturbation of metal binding to the target protein is monitored. By knowing log K_{app1} of the metal ion:chelator complex, log K_{app} of the protein:metal ion complex can be deduced. If log K_{app1} > log K_{app2}, then metal ion will bind protein > chelator. If log K_{app1} < log K_{app2}, then metal ion will bind protein < chelator. If log K_{app1} = log K_{app2}, then metal ion will bind protein and chelator equally. Therefore, at half-maximal binding of metal ion to protein, reflected by shifts in protein: metal stoichiometry or other physicochemical changes, e.g., solubility, log K_{app1} = log K_{app2}.

apparent Aβ1–40 dimer by Cu^{2+} on gel chromatography (Bush et al., 1994*a*) and by the displacement of $^{65}Zn^{2+}$ from Aβ when coincubated with excess Cu^{2+} (Clements et al., 1996). We recently demonstrated that Cu^{2+} binds to soluble Aβ via histidine residues and that the precipitation of soluble Aβ by Cu^{2+} is reversibly modulated by pH; mildly acidic conditions (pH 6.6) greatly promote Cu^{2+}-mediated precipitation, whereas alkalinization resolubilizes precipitated Aβ:Cu^{2+} complexes (Atwood et al., 1998). The roles these metal ions play in cerebral amyloid assembly were demonstrated from experiments showing that Cu^{2+}- and Zn^{2+}-selective chelators enhance the solubilization of Aβ collections in postmortem brain specimens from AD subjects (Cherny et al., 1999) and from amyloid precursor protein transgenic mice (Gray et al., 1998).

Our previous study (Atwood et al., 1998) using indirect spectrophotometric analysis of Cu^{2+} binding to Aβ indicated half-maximal binding of Cu^{2+} for Aβ in the micromolar range (4.0 μ*M* for Aβ1–40 and 0.3 μ*M* for Aβ1–42). However, this analysis of binding affinities was limited by the sensitivity of the spectrophotometric technique and the lack of competitive binding factors in the incubation that would emulate the physiological situation more closely. Given the potential importance of Aβ:Cu^{2+} interactions to the pathophysiology of amyloid deposition (Atwood et al., 1998; Cherny et al., 1999), we sought alternative strategies to characterize more precisely the multiple Cu^{2+} binding sites on Aβ. Because of the hazards and inconveniences of working with metal radioisotopes, the inherent difficulties in describing multiple equilibria for metal complexes of proteins involving affinities over a very broad range of values, and especially the tendency of Aβ peptides to precipitate in the presence of metal ions, we developed a competitive metal capture analysis (CMCA) ligand displacement technique (Fig. 1) using metal–chelator complexes for the determination of stoichiometry and estimation of binding affinities of multiple Cu^{2+} (and Zn^{2+}) ions to proteins. The use of metal:chelator complexes approximates the in vivo exchange of a metal ion from one protein or ligand to another. CMCA also circumvents concerns that metal ions added as simple salts may hydrolyze, in a pH-dependent manner, to form metal–hydroxy and –oxy polymers, which may either bind nonspecifically to the protein or become biologically inert (Spiro and Saltman, 1969).

CMCA revealed that (a) Aβ remains soluble provided that it is prevented from binding Cu^{2+}, (b) multiple affinity cooperative Cu^{2+} binding sites exist on Aβ, but Aβ1–42 exhibits much stronger cooperative binding than Aβ1–40, which is especially reflected at the highest affinity site, (c) Aβ binds equimolar amounts of Cu^{2+} and Zn^{2+} at pH 7.4, but Cu^{2+} displaces Zn^{2+} from Zn^{2+}:Aβ complexes under acidic conditions (pH 6.6), (d) Aβ1–42 markedly precipitates in the presence of trace amounts (<0.1 μ*M*) of metal ions, (e) Cu^{2+} induces sodium dodecyl sulfate (SDS)-resistant oligomerization of Aβ (Aβ1–42 > Aβ1–40), and (f) chelators both inhibit and reverse Cu^{2+}-mediated precipitation of Aβ1–42. Our data also reveal that the high-affinity binding of Cu^{2+} to Aβ1–42 promotes precipitation and that this affinity is so high that it is hard to avoid self-aggregation in normal buffers. These results imply that extremely small changes in free or exchangeable Cu^{2+} concentration may have an impact on Aβ solubility in vivo.

EXPERIMENTAL PROCEDURES

Reagents and preparation

Human Aβ1–40 and Aβ1–42 peptides were synthesized, purified, and characterized by HPLC analysis, amino acid analysis, and mass spectroscopy by the W. M. Keck Foundation Biotechnology Resource Laboratory (Yale University, New Haven, CT, U.S.A.). The HPLC elution profiles of the peptides were identified as a single peak. Synthetic Aβ peptide solutions were dissolved in Milli-Q water (Millipore Corp., Milford, MA, U.S.A.) at a concentration of 0.5–1.0 mg/ml and centrifuged for 10 min at 10,000 *g*, and the supernatant (stock Aβ) was used for subsequent precipitation and metal binding assays on the day of the experiment. Metal ion analyses (see below) indicated ≈0.04 μ*M* Cu or Zn per 1 μ*M* Aβ. The concentration of stock Aβ peptides was determined by spectrophotometric absorbance at 214 nm (against calibrated standard curves). Dog serum albumin (DSA; Sigma Chemical Co., St. Louis, MO, U.S.A.) was prepared in deionized water to a stock concentration of 10 mg/ml. Metal ion analyses (see below) indicated a small quantity of Cu (≈0.04 μ*M* per 1 μ*M* DSA) but no Zn in DSA stock solutions. Chelators and other reagents were purchased from Sigma and Aldrich Chemical Co. (Milwaukee, WI, U.S.A.). Metal ion stock solutions were prepared by mixing National Institute of Standards and Technology metal standards [Cu^{2+} (10 mg/ml) in 10% HNO_3, standard reference material no. 3114; Zn^{2+} (10 mg/ml) in 10% HCl, standard reference material no. 3168] to the desired concentration in doubly deionized water. The low concentration of metal ion used in the assays (50 μ*M*) introduced a small quantity of acid into the reaction mixture. However, the acid dilution was so great that it did not alter the pH of the buffered reaction mixtures, which were measured both before and after addition of metal ion: chelator complex. Before use all buffers and stock solutions of metal ions were filtered (pore size, 0.22 μm; Gelman Sciences, Ann Arbor, MI, U.S.A.) to remove any particulate matter.

TABLE 1. *Log K_{app} of Cu^{2+}- and Zn^{2+}-selective chelators*

	Cu^{2+} log K_{app}				Zn^{2+} log K_{app}		
Chelator	pH 7.4	pH 7.0	pH 6.6	Chelator	pH 7.4	pH 7.0	pH 6.6
Tris	1.8	1.4	1.0	Tris	3.2	2.8	2.4
Glycine	5.9	5.5	5.1	Bicine	4.7	4.3	3.9
Arginine	5.9	5.5	5.1	Histidine	5.0	4.5	4.2
Methionine	6.3	5.9	5.5	ACES	5.0	4.6	4.2
Asparagine	6.6	6.2	5.8	Citric acid	5.3	4.9	4.5
Histamine	7.2	6.8	6.4	Bipyridyl	5.8	5.4	5.0
Bicine	7.4	7.0	6.6	Tricine	6.5	6.1	5.7
Ethylenediamine	7.8	7.4	7.0	HIMDA	7.1	6.7	6.3
Histidine	8.4	8.0	7.8	NTA	8.0	7.6	7.2
Bipyridyl	8.9	8.5	8.1	EGTA	10.0	9.6	9.2
HIMDA	10.6	10.2	9.8				
EDDA	14.1	13.7	13.3				
EDTA	15.9	15.5	15.1				
DTPA	16.3	15.9	15.5				
CDTA	17.0	16.6	16.2				

ACES, *N*-(carbamoylmethyl)-2-aminoethanesulfonic acid; bicine, *N,N*-bis(2-hydroxyethyl)glycine; bipyridyl, 2,2′-dipyridyl; EDDA, ethylenediamine-*N,N*′-diacetic acid; HIMDA, *N*-(2-hydroxyethyl)iminodiacetic acid; NTA, nitrilotriacetic acid; Tricine, *N*-tris(hydroxymethyl)methylglycine.

Determination of apparent log *K* from absolute log *K*

Metal ion chelators were chosen from the National Institute of Standards and Technology Standard Reference Database 46 (Critically Selected Stability Constants of Metal Complexes Database, version 4.0; U.S. Department of Commerce) and other reference databases (Dawson et al., 1986). Chelators were chosen to give a range of stability constants at approximately half log order intervals. Stability constants ($K = [ML]/[M][L]$, where M = metal ion and L = ligand) chosen for metal: chelators were for 25°C, an ionic strength of 0.1–0.2 υ, and a molar ratio of chelator to metal ion of 1:1. Where more than one complex is formed between a metal ion and a chelator, a chelator was only elected if the log K of its metal:chelator complex with a ratio of 1:1 was the greatest of all possible complexes.

The log K of a chelator for metal ions is affected by the pH of the solution as determined by the following equations [after Ringblom (1963) and Schwarzenbach and Flaschka (1969)]:

$$\log K_{\text{apparent}} = \log K - \log \alpha$$

where

$$\alpha = \frac{[H^+]_n}{K_{a1} * K_{a2} * K_{a3} * \ldots K_{an}} + \frac{[H^+]_{n-1}}{K_{a1} * K_{a2} * \ldots K_{an-1}} + \cdots + \frac{[H^+]}{K_{a1}} + 1$$

$K_a = 10^x$, where $x = -pK_a$ of the chelator (K_a values are listed in order of decreasing pK_a values), and n = no. of pK_a values. Values for log K_{app} for chelators used at pH 7.4, 7.0, and 6.6 are presented in Table 1.

Stoichiometry and binding analyses of metal ions for Aβ and DSA

Solutions of metal:chelator were prepared in a ratio of 1:2 (5 m*M*:10 m*M*) in doubly deionized water and allowed to come to equilibrium for 24 h at room temperature. Samples containing Aβ (10 μ*M*) or DSA (10 μ*M*) with and without metal ion: chelator complexes (50 μ*M* metal ion, 100 μ*M* chelator), along with background controls of protein plus chelator (no metal) or metal:chelator alone, were prepared in 20 m*M* Tris/150 m*M* NaCl buffer at pH 7.4 and 6.6 (for Aβ) and pH 7.0 (for DSA) to a final volume of 1 ml and incubated for 24 h at 37°C. Tris was chosen as the buffer because it only weakly complexes Cu ions and its log K_{app} has been characterized (Dawson et al., 1986). The value of pH 6.6 was chosen as a condition of severe acidosis and also to make comparisons with our previous publication.

Following incubation the sample was split into three fractions: Fraction 1 was used to confirm the initial concentrations of total protein [150 μl for Micro BCA assay (Pierce, Rockford, IL, U.S.A.)] and total metal ion (150 and 20 μl for Cu and Zn assays, respectively) in the reaction samples. Fraction 2 (330 μl) was loaded into a 3-kDa cutoff filter (Concentrator; Amicon, Beverly, MA, U.S.A.) and centrifuged at 10,000 *g* for 30–45 min, and the filtrate, which contained no peptide, was collected for metal ion analysis (20 μl for Zn and 160 μl for Cu). Fraction 3, the remainder of the reaction sample (330 μl), was centrifuged for 10 min at 10,000 *g*, and the supernatant was assayed for soluble protein and metal ion concentrations from which the respective concentrations in the pellet could be deduced. We have previously shown that centrifugation of Aβ solutions at 10,000 *g* for 10 min sediments all precipitated Aβ compared with ultracentrifugation at 100,000 *g* for 1 h (Atwood et al., 1998). As DSA did not precipitate in the presence of Zn^{2+} or Cu^{2+}, reaction mixtures of DSA and metal ions were divided into fractions 1 and 2 for assay. Appropriate blank samples (buffer with or without Aβ, buffer with or without metal ion) also were analyzed for background readings.

Scatchard analysis

Having assayed the amount of protein-bound metal ion in the incubation, the remaining metal ion in the non–protein-bound fraction is in an equilibrium between being free and being bound to the chelator. Therefore, the free concentration of metal ion could be calculated using the chelator stability constant for the metal ion applied to this fraction. Scatchard linearization analysis was only performed on data where the

metal-bound protein fraction was >4% of total available metal. Where the Scatchard plot revealed multiple binding affinities, the lowest and the highest binding affinities were calculated from the slope of the asymptotes of the data points in the high- and low-affinity regions. Where the Scatchard analysis indicated an accelerating regression curve, a further plot of [log(Aβ-bound Cu^{2+} concentration)]/free Cu^{2+} concentration versus Aβ-bound Cu^{2+} concentration was performed, and the linear regression coefficient was determined. The slope of this line correlates with the cooperative binding coefficient.

Protein and metal ion assays

Protein concentration was determined using the Micro BCA Assay, as previously described (Atwood et al., 1998). Standard curves for the Micro BCA protein assay were determined to be linear in the range of Aβ concentrations studied (0–10 μ*M*). There was close agreement between the quantities of Aβ in a sample (n = 6) of unprecipitated and filterable fractions from our Cu^{2+}-induced precipitation studies when assayed by Micro BCA assay, compared with amino acid analysis values. However, the Micro BCA assay detected ~15% less Aβ in a resuspension (in phosphate-buffered saline, pH 7.4) of precipitated peptide than the levels in the same sample measured by amino acid analysis. Therefore, we chose to measure the depletion of unprecipitated and filterable Aβ as an index of peptide precipitation.

The concentration of total Zn^{2+} ("total" = chelator- or protein-bound metal ion + free metal ion) was determined using the spectrophotometric method of Makino (1991). To 20 μl of sample, 100 μl of GTAC solution (7 *M* guanidine HCl, 0.4 *M* Tris, 10 m*M* ascorbic acid, and 5 m*M* sodium cyanide, pH 8.1) was added to each well of a 96-well microtiter plate (Corning Costar, Corning, NY, U.S.A.), and the plate was mixed continuously for 1 min. Following incubation at room temperature for 5 min, chloral hydrate solution (1 *M*; 25 μl) and 2-(5-nitro-2-pyridylazo)-5-(*N*-propyl-*N*-sulfopropylamino)phenol (0.3 mg/ml, 25 μl) were added to the plate, which was then mixed for 1 min, and the absorbance was read at 574 nm.

The concentration of total ionic Cu was determined using the spectrophotometric method of Matsuba and Takahashi (1970), adapted to microwell plate volumes, as previously described (Atwood et al., 1998). The standard curves for Cu^{2+} and Zn^{2+} assays were demonstrated to be unaffected by the presence of any of the chelators or proteins that we investigated, indicating that the metal ion detection reagents were reacting equally with the metal ions in both their bound and free states. Standard curves for the metal assays were determined to be linear in the range of the metal concentrations studied (0–50 μ*M*).

Determination of soluble and precipitated protein

The percent precipitation of Aβ was determined after centrifugation of the samples (fraction 3) and removal of the supernatant for analysis using the Micro BCA protein assay using the following formulas:

$$\%\ \text{Soluble A}\beta = \frac{(\text{absorbance of supernatant fraction} - \text{absorbance of blank})}{(\text{absorbance of initial} - \text{absorbance of blank})} \times 100$$

$$\%\ \text{Precipitated A}\beta = 100 - \%\ \text{soluble A}\beta$$

After incubation, it is possible that the Aβ may have formed soluble multimers; however, for simplicity the concentration of Aβ was expressed as equivalent concentrations of Aβ monomer in solution.

Determination of Zn^{2+}/Cu^{2+} concentration

The concentrations of total Zn^{2+} and Cu^{2+} in the 3-kDa filtrate fraction (fraction 2) and in the supernatant fraction (fraction 3) were measured directly. The total soluble metal ion concentration ($[M^{2+}]_{soluble}$) and non–peptide-bound metal ion concentration ($[M^{2+}]_{non\text{–}peptide\text{-}bound}$), reflecting free plus chelator-bound metal ions, were determined using the following formulas:

$$[M^{2+}]_{soluble} = \frac{[\text{absorbance of supernatant fraction (fraction 3)} - \text{absorbance of blank}]}{(\text{absorbance of initial} - \text{absorbance of blank})} \times [M^{2+}]_{initial}$$

$$[M^{2+}]_{non\text{–}peptide\text{-}bound} = \frac{[\text{absorbance of filtrate fraction (fraction 2)} - \text{absorbance of blank}]}{(\text{absorbance of initial} - \text{absorbance of blank})} \times [M^{2+}]_{initial}$$

The initial total metal ion concentration was 50 μ*M* (see above).

The stoichiometry of metal ion binding to total Aβ (both soluble and precipitated), soluble Aβ, and precipitated Aβ was subsequently determined using the following equations:

$$\text{Ratio of metal bound to total A}\beta\ \text{(both soluble and precipitated)} = \frac{[M^{2+}]_{initial} - [M^{2+}]_{non\text{–}peptide\text{-}bound}}{[A\beta]_{initial}}$$

$$\text{Ratio of metal bound to soluble A}\beta = \frac{[M^{2+}]_{soluble} - [M^{2+}]_{non\text{–}peptide\text{-}bound}}{[A\beta]_{soluble}}$$

$$\text{Ratio of metal bound to precipitated A}\beta = \frac{[M^{2+}]_{initial} - [M^{2+}]_{soluble}}{[A\beta]_{initial} - [A\beta]_{soluble}}$$

A candidate binding site was also evidenced by a discrete shift in the stoichiometric bound metal:Aβ ratio. A change in stoichiometry was sometimes accompanied by a discrete change in solubility that was taken as further support of a binding site. The affinity of the binding site was also estimated by the corresponding log K_{app} of the competing metal:chelator complex, at which point the half-maximal shift in stoichiometry or solubility was identified.

DSA did not aggregate under the current reaction conditions, and bound metal concentrations were determined as described above for Aβ (initial [*M*] − non–protein-bound [*M*]).

Inhibition of Aβ precipitation

Aβ1–40 or Aβ1–42 (10 μ*M* each) was incubated in phosphate-buffered saline (pH 7.4) with or without diethylenetriaminepentaacetic acid (DTPA; 200 μ*M*) for 5 days at 37°C, and then the turbidity of the solution was measured at 405 nm. In another experiment Aβ1–42 (5 μ*M*) was induced to aggre-

gate by incubation in 20 m*M* Tris/150 m*M* NaCl buffer at pH 7.4 or 6.6 with $CuCl_2$ (20 μM) for 1 h at 37°C. Following precipitation, samples were incubated with no chelator, EDTA, or DTPA (200 μM each) for 1 h at 37°C. Samples were then centrifuged (10,000 *g* for 20 min), and the supernatant was analyzed for protein concentration to determine percent total peptide in the soluble fraction as previously described (Atwood et al., 1998).

Competition analyses of zinc and copper for Aβ

Aβ1–40 (10 μM) was incubated in 20 m*M* Tris/150 m*M* NaCl buffer at pH 7.4 or 6.6 with $ZnCl_2$, $Cu(NO_3)_2$, or $ZnCl_2$ plus $Cu(NO_3)_2$ (50 μM each) for 48 h or $ZnCl_2$ (50 μM) for 24 h, and then $Cu(NO_3)_2$ (50 μM) was added for a further 24 h. Following incubation, samples were analyzed for percent precipitation and stoichiometry of metal ion binding to Aβ as described above.

SDS-resistant polymerization of Aβ

Aβ stock solutions were diluted to 2.5 μM in phosphate-buffered saline (66 m*M* phosphate and 150 m*M* NaCl, pH 7.4) and incubated with or without $CuCl_2$ (30 μM) for 0 and 1 day at 37°C. Aliquots of each reaction mixture (2 ng of peptide) were collected into 15 μl of sample buffer (containing 4% SDS and 5% β-mercaptoethanol) and heated to 95°C for 5 min. Samples were loaded, electrophoresed on polyacrylamide gel electrophoresis (PAGE; Tricine gels, 10–20%; Novex, San Diego, CA, U.S.A.) at 25°C and pH 8.45, transferred to polyvinylidene difluoride membranes (Bio-Rad Laboratories, Hercules, CA, U.S.A.), fixed with glutaraldehyde (1%, vol/vol), blocked with milk (10%, wt/vol), and then probed with anti-Aβ monoclonal antibody 6E10 (or 4G8; Senetek, Maryland Heights, MI, U.S.A.) overnight at 4°C. The blot was then incubated with anti-mouse horseradish peroxidase conjugate (Pierce) for 2 h at room temperature and developed with ECL reagent (1 min; Amersham, Little Chalfont, Bucks, U.K.) or Supersignal Ultra (5 min; Pierce) following the manufacturer's instructions. The chemiluminescent signal was captured on film or for 10 min at maximal sensitivity using the Fluoro-S Image Analysis System (Bio-Rad). Electronic images were analyzed using Multi-Analyst Software (Bio-Rad). Molecular size markers were from Amersham (Arlington Heights, IL, U.S.A.).

RESULTS

Stoichiometry and estimated binding affinities of Cu^{2+} and Zn^{2+} for DSA

We developed a method (CMCA) to enable the determination of stoichiometry of metal ion binding to both soluble and precipitated forms of Aβ and to permit an estimation of metal ion binding affinities to Aβ (Fig. 1). To validate this methodology, we first studied a protein with known Cu^{2+} and Zn^{2+} binding affinities (DSA) (Fig. 2). DSA was found to bind on average ~2 Zn^{2+} (1.7 ± 0.2; mean ± SD) in the presence of Zn^{2+}:chelator complexes with log K_{app} values of ≤6.2 at pH 7.0 (Fig. 2A). Scatchard analysis of Zn^{2+} binding to DSA indicated that there was a single affinity binding site ($K_D = 1.3 \times 10^{-7}$ *M*, log K_{app} = 6.9) binding both Zn^{2+} ions (Fig. 2B), in agreement with previously reported values (Masuoka et al., 1993).

DSA also bound ~2 Cu^{2+} ions (1.7 ± 0.1; mean ± SD) when incubated in the presence of Cu^{2+}:chelator

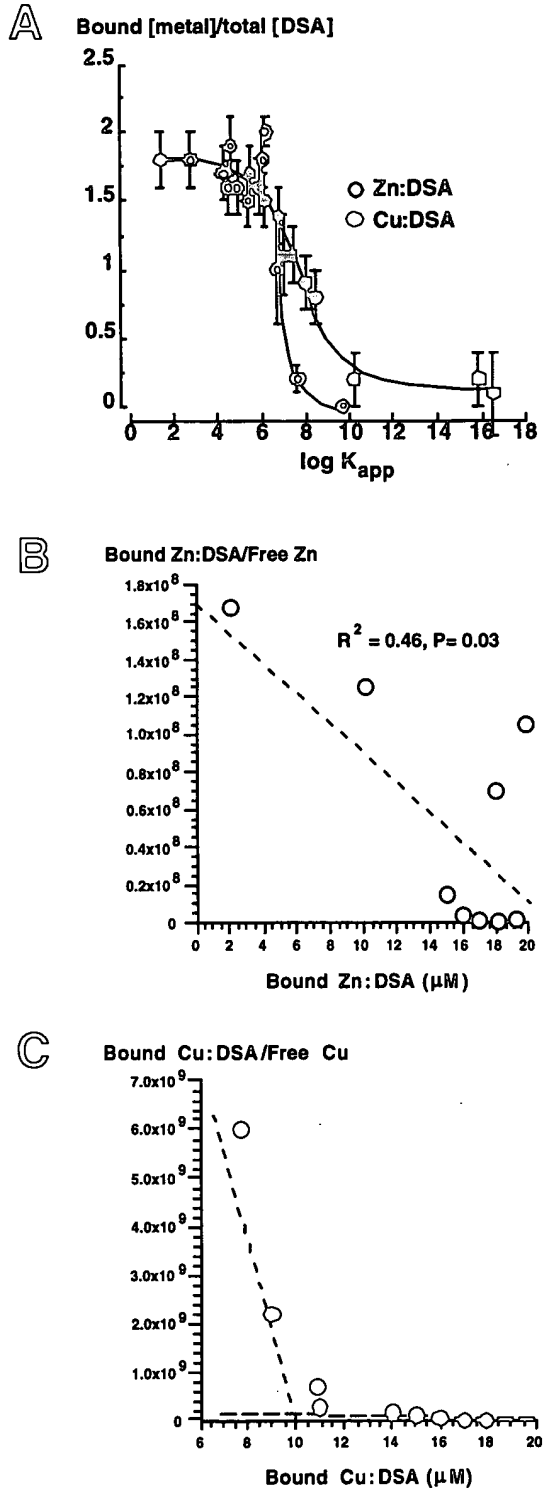

FIG. 2. CMCA of Cu and Zn binding to DSA. **A:** DSA (10 μM) was incubated with metal:chelator complexes (50 μM) for 24 h, and the stoichiometry of binding was determined. Data are mean ± SD (bars) values (n = 6). **B** and **C:** Scatchard analysis of the data in A.

complexes with log K_{app} of ≤5.9 at pH 7.0 (Fig. 2A and C). In the presence of Cu^{2+}:chelator complexes with log K_{app} of >5.9, the stoichiometry of Cu^{2+}:DSA binding gradually decreased. Scatchard analysis (Fig. 2C) of the binding data indicated two Cu^{2+} binding sites: one with a lower affinity ($K_D = 2.2 \times 10^{-8}$ *M*, log $K_{app} = 7.7$) and one with a higher affinity ($K_D = 6.2 \times 10^{-10}$ *M*, log $K_{app} = 9.2$). The estimate of the high-affinity Cu binding site is in reasonable agreement with that of Masuoka et al. (1993), who observed a high-affinity binding site for Cu with log K_{app} of 10.17. Our finding that DSA binds 1.7 atoms of Zn^{2+} and 1.7 atoms of Cu^{2+} at pH 7.0 (Fig. 2) is in agreement with previous studies suggesting that DSA may have multiple Cu^{2+} (Appleton and Sarkar, 1971) and Zn^{2+} (Goumakos et al., 1971) binding sites. Taken together, these results suggest that our methodology is a valid approach for the estimation of stoichiometry and binding affinities of metal ions for proteins.

Relationship among Aβ:Cu stoichiometry, binding affinity, and precipitation

We next assessed the stoichiometry and affinities of Cu^{2+} binding to total Aβ present (soluble and precipitated forms). At pH 7.4, Cu^{2+} binding to Aβ1–40 and Aβ1–42 saturated at 1.8 ± 0.1 and 2.2 ± 0.1 bound Cu^{2+} ions, respectively, in the presence of Cu^{2+}:chelator complexes of log K_{app} of ≤6.6 (Fig. 3A). As the log K_{app} of the array of Cu^{2+}:chelator complexes was increased above 6.6, the stoichiometry of Cu^{2+}:Aβ binding decreased (Fig. 3A and C). Scatchard analysis (Fig. 3E and insets) indicated that the Aβ peptides both possess multiple cooperative Cu^{2+} binding sites at either pH 7.4 or 6.6. At pH 7.4, the lowest-affinity Cu^{2+} binding site for Aβ1–40 ($K_D = 1.3 \times 10^{-8}$ *M*, log $K_{app} = 7.9$; Fig. 3A and E and Table 2) saturated at a stoichiometry of 2 Cu^{2+}. The K_D of the highest-affinity Cu^{2+} binding site on Aβ1–40 was difficult to determine by Scatchard analysis because of insufficient data points in the high-affinity range to get an accurate regression line. However, we observed that the curve of the Scatchard plot exhibited concave acceleration and that log plots of the Scatchard analyses (Fig. 3E, insets) were significantly linear, indicating negative cooperativity of multiple Cu^{2+} binding sites on Aβ (Fig. 3E, insets). Therefore, using the linear relationship between log(bound $[Cu^{2+}]$/free $[Cu^{2+}]$) and bound $[Cu^{2+}]$, we could still estimate the affinity of high-affinity Cu^{2+} binding site on Aβ1–40 as 4.6×10^{-11} *M*, log $K_{app} = 10.3$, if the stoichiometry of Cu^{2+} binding to this site is assumed to be the same as that for the Aβ1–42 high-affinity site (0.5; Fig. 3E and Table 2).

Aβ1–42 was observed to have a similar affinity for Cu^{2+} (2 equivalents) at its lowest-affinity binding site compared with Aβ1–40 at pH 7.4 ($K_D = 5.0 \times 10^{-9}$ *M*, log $K_{app} = 8.3$; Fig. 3A and E and Table 2). However, Aβ1–42 possesses a much greater affinity for Cu^{2+} (0.5 equivalents) at its highest-affinity site ($K_D = 7.0 \times 10^{-18}$ *M*, log $K_{app} = 17.2$; Fig. 3A and E and Table 2) than Aβ1–40 at pH 7.4. The Scatchard analysis of Cu^{2+} binding to Aβ1–42, as well as the log-linearization of the Scatchard plot (Fig. 3E, insets), provided sufficient data in the high-affinity range for an accurate estimation of the affinity of this site.

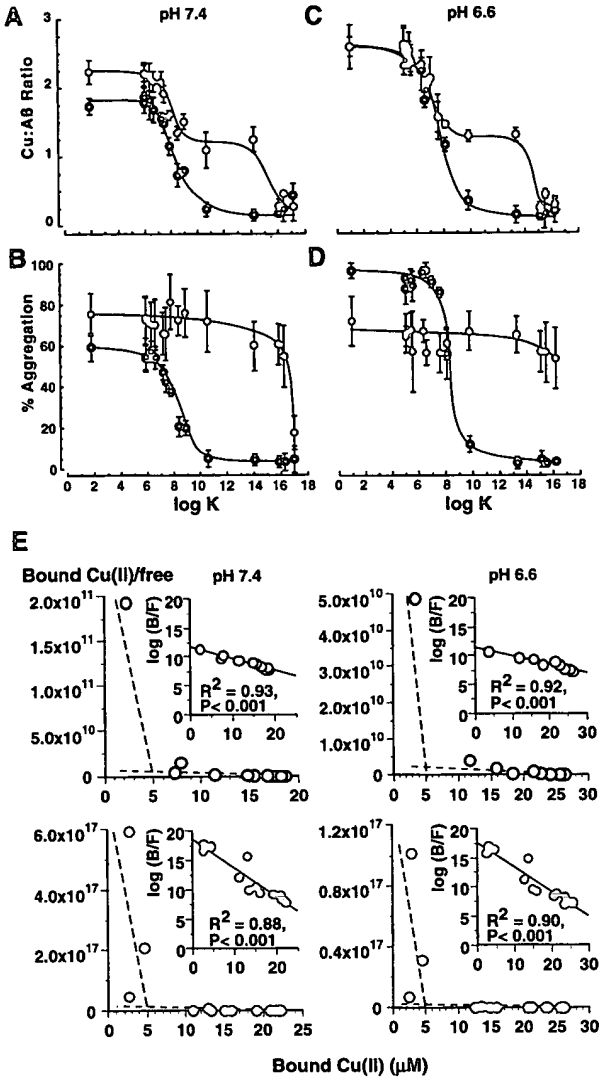

FIG. 3. CMCA of Cu^{2+} binding and precipitation of total Aβ. The ratio (Cu:Aβ) of bound Cu^{2+} to Aβ (soluble and precipitable forms) and the corresponding percentage of Aβ precipitation are plotted against log K_{app} of the competing Cu^{2+}:chelator complex. Aβ1–40 (○) or Aβ1–42 (○) (10 µ*M*) was incubated at pH 7.4 and 6.6 with an array of Cu^{2+}:chelator complexes (50 µ*M* Cu^{2+}) for 24 h, and the precipitation and stoichiometry of metal ion binding to total Aβ were determined. Data are mean ± SD (bars) values (n = 4–6) **A:** Bound Cu^{2+}:Aβ ratio at pH 7.4. **B:** Cu^{2+}-induced Aβ precipitation at pH 7.4. **C:** Bound Cu^{2+}:Aβ ratio at pH 6.6. **D:** Cu^{2+}-induced Aβ precipitation at pH 6.6. Suggested curves have been fitted to the data for purposes of clarity. **E:** Scatchard analyses of the data in A and C. The asymptotes of the fitted curves are shown, whose slopes reflect $-1/K_D$ for the highest- and lowest-affinity Cu^{2+} binding sites. **Insets:** Same Scatchard analyses with logarithmic treatment of the *y*-axis [log(*B*/*F*)]/*B* to demonstrate the acceleration of the Scatchard curves (regression coefficients and *p* values shown), implying multiple cooperative Cu^{2+} binding sites on Aβ. *B*, bound; *F*, free.

Unlike Aβ1–40, Aβ1–42 was >60% precipitated when incubated with each of the Cu^{2+}:chelator com-

TABLE 2. *Summary of binding affinities (log K_{app}) for Cu^{2+} binding to Aβ1–40 and Aβ1–42*

	Aβ1–40		Aβ1–42				
	log K_{app}	Stoichiometry of Cu:Aβ	log K_{app}	Stoichiometry of Cu:Aβ			
pH 7.4							
Highest affinity	10.3	0.5	17.2	0.5			
Lowest affinity	7.9	2	8.3	2			
	Slope [log(*B*/*F*)]/*B*	R^2	Slope [log(*B*/*F*)]/*B*	R^2	*t*	*df*	*p*
	−0.20	0.93	−0.50	0.88	2.98	44	0.002
pH 6.6							
Highest affinity	9.6	0.5	16.3	0.5			
Lowest affinity	7.0	2.5	7.5	2.5			
	Slope [log(*B*/*F*)]/*B*	R^2	Slope [log(*B*/*F*)]/*B*	R^2	*t*	*df*	*p*
	−0.15	0.92	−0.42	0.90	3.03	44	0.002

The data in Fig. 3 for Cu^{2+} binding to Aβ were analyzed and are summarized here. Log K_{app} values are derived from the slopes of the Scatchard plots in Fig. 3E, and the estimated stoichiometries of Cu^{2+} binding to the highest- and lowest-affinity sites are derived from the estimated *x*-axis intercepts in Fig. 3E. The slope of the analysis of [log(*B*/*F*)]/*B* derived from the insets of Fig. 3E is shown, along with the regression coefficients of these slopes, reflecting cooperative binding of Cu^{2+} to Aβ. The slope of [log(*B*/*F*)]/*B* for Cu^{2+} binding to Aβ1–42 is significantly greater than the slope of [log(*B*/*F*)]/*B* for Cu^{2+} binding to Aβ1–40 [*t* test value, degrees of freedom (*df*), and *p* values are shown]. This indicates that there is significantly greater cooperative binding of Cu^{2+} to Aβ1–42 compared with Aβ1–40.

plexes except in the presence of the chelator with the highest affinity for Cu^{2+} [*trans*-1,2-diaminocyclohexane-*N*,*N*,*N*′,*N*′-tetraacetic acid (CDTA), log K_{app} = 17.0], when the solubility of the peptide abruptly and dramatically increased (Fig. 3B). The possibility of CDTA directly binding to Aβ1–42 and acting as a chain breaker was excluded by nuclear magnetic resonance spectroscopy studies (X. Huang, K. Barnham, C. S. Atwood, R. E. Tanzi, and A. I. Bush, unpublished data).

At pH 6.6, the stoichiometry of low-affinity Cu^{2+} binding to both peptides increased (Fig. 3C). At pH 6.6, Aβ1–40 and Aβ1–42 bound 0.8 and 0.3 more Cu^{2+} ions (2.6 ± 0.1 and 2.5 ± 0.1, respectively) than at pH 7.4 in the presence of Cu^{2+}:chelator complexes in lower-affinity range (log K_{app} < 7.8), so that the stoichiometry of Cu^{2+} binding to Aβ1–40 approached that of Aβ1–42 (Fig. 3C). At pH 6.6, the affinity of the lowest-affinity Cu^{2+} binding site estimated by Scatchard analysis (Fig. 3E) decreased for both Aβ1–40 and Aβ1–42 (Aβ1–40, $K_D = 9.3 \times 10^{-8}$ *M*, log K_{app} = 7.0; Aβ1–42, $K_D = 3.3 \times 10^{-8}$ *M*, log K_{app} = 7.5; Table 2), compared with the affinity at pH 7.4. There was no significant change in Cu^{2+}:Aβ stoichiometry after incubation with Cu^{2+}:chelator complexes in the high-affinity range (log K_{app} = 7.8–16.2) at pH 6.6 compared with the values at pH 7.4. There was an accompanying decrease of ≈1 log unit in the estimated log K_{app} values for the high-affinity Cu^{2+} binding sites for both Aβ1–40 ($K_D = 2.6 \times 10^{-10}$ *M*, log K_{app} = 9.6; Table 2) and Aβ1–42 ($K_D = 4.5 \times 10^{-17}$ *M*, log K_{app} = 16.3; Table 2) at pH 6.6 (Fig. 3C and E), compared with the corresponding values at pH 7.4 (Fig. 3A and E).

The slope of the plot of log(bound [Cu^{2+}]/free [Cu^{2+}]) and bound [Cu^{2+}] (Fig. 3E, insets) correlates with the cooperativity coefficient for the multiple Cu^{2+} binding sites on Aβ. We found that at either pH 6.6 or 7.4, this slope was significantly (≈2.5-fold, $p = 0.002$) greater for Cu^{2+} binding to Aβ1–42 than for binding to Aβ1–40 (Fig. 3E and Table 2). This means that the acceleration of the Scatchard plot was 2.5-fold greater for Cu^{2+} binding to Aβ1–42, indicating that Aβ1–42 has markedly greater cooperative binding of Cu^{2+} than Aβ1–40.

The increase in low-affinity Cu^{2+} binding to Aβ1–40 induced by incubation at the lower pH (6.6) correlated with a ≈30% increase in Aβ1–40 precipitation (Fig. 3D) compared with that induced at pH 7.4 (Fig. 3B). However, although the incubation at pH 6.6 increased low-affinity Cu^{2+} binding to Aβ1–42, precipitation of Aβ1–42 at the lower pH (Fig. 3D) was not increased compared with precipitation at pH 7.4 (Fig. 3B).

Although at pH 7.4 CDTA did not permit sufficient Cu^{2+} to bind to Aβ1–42 to induce peptide precipitation (Fig. 3B), at pH 6.6 incubation of Aβ1–42 with CDTA:Cu^{2+} complexes was accompanied by ≈50% precipitation of Aβ1–42 (Fig. 3D). Note, however, that CDTA and all of the chelator array have lower Cu^{2+} binding affinities at the lower pH; the log K_{app} of CDTA for Cu^{2+} decreases from 17.0 at pH 7.4 to 16.2 at pH 6.6 (Table 1).

Taken together, these findings indicate that Aβ1–40 and Aβ1–42 precipitate if bound to 1 Cu^{2+}. Conversely, Aβ1–40, and even Aβ1–42 (at pH 7.4), will remain soluble if Cu^{2+} binding is totally prevented.

Although there was a strict correspondence between the stoichiometry of bound Cu^{2+} and the amount of Aβ1–40 precipitation (r^2 = 0.89 at pH 7.4 and 0.85 at pH 6.6; Fig. 4), there was a weak correlation (and at pH 6.6, no correlation) between the stoichiometry of bound Cu^{2+} and the amount of Aβ1–42 precipitation (r^2 = 0.17 at pH 7.4 and r^2 = 0.09 at pH 6.6; Fig. 4). The change in pH from 7.4 to 6.6 did not alter the slope of the linear relationship between Cu^{2+}:Aβ1–40 stoichiometry and precipitation (Fig. 4), which indicates that the Cu^{2+} binding to Aβ1–40 saturates at 2.5 Cu^{2+} ions.

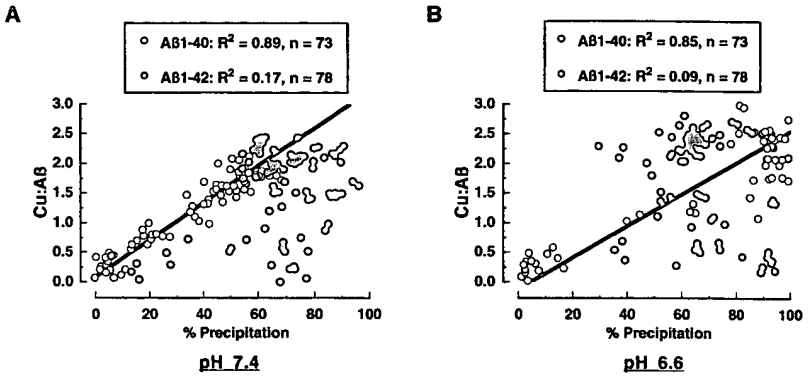

FIG. 4. Correlation of the stoichiometric ratio of Cu:Aβ1–40 (○) and Cu:Aβ1–42 (○) with peptide precipitation. Precipitation is expressed as a percentage of total peptide. **A:** Cu:Aβ ratio at pH 7.4. **B:** Cu:Aβ ratio at pH 6.6. Linear regression equations are shown where x = percent precipitation and y = metal:Aβ ratio.

Stoichiometry of Aβ binding to soluble and precipitated Aβ fractions

The stoichiometry values determined from the data in Fig. 3 represent binding of Cu^{2+} to Aβ peptides that exist in a mixture of soluble and precipitated forms in an equilibrated incubation mixture. Therefore, these values represent averages that depend on the stoichiometries of Cu^{2+} binding to the respective soluble and precipitated components of the mixture, as well as the proportions of each component. To study the stoichiometry of Cu^{2+} binding to these individual components, Aβ peptides were incubated with the array of Cu^{2+}:chelator complexes and centrifuged, and the stoichiometries of metal binding were determined for the peptide fractions in the supernatant (soluble Aβ) and pellet (precipitated Aβ) under conditions where the peptide was maximally soluble or maximally precipitated (Table 3).

When the total Aβ/Cu^{2+} mixture was predominantly (>80%) soluble at pH 7.4, the soluble Aβ1–40 and Aβ1–42 components bound close to zero Cu^{2+} ions (Table 3 and Fig. 3). When the total Aβ1–40/Cu^{2+} mixture was predominantly (>80%) soluble at pH 6.6, the soluble Aβ1–40 component also bound close to zero Cu^{2+} ions (Table 3 and Fig. 3). The total Aβ1–42/Cu^{2+} mixture was never predominantly soluble at pH 6.6 under the conditions tested, even in the presence of the highest-affinity Cu^{2+} chelator (CDTA), so the stoichiometry of Cu^{2+} bound to the soluble Aβ1–42 component was determined as 0.30 under conditions where the mixture was least precipitated (53.1% at log K_{app} = 16.2; Table 3).

Under conditions of maximal Cu^{2+}-induced precipitation (Fig. 3), the stoichiometry of Cu^{2+} binding within Aβ1–40–Cu and Aβ1–42–Cu precipitates at pH 7.4 was both ~2.5 (Table 3). The stoichiometry of Cu^{2+} binding to maximally precipitated Cu^{2+}:Aβ1–40 complexes at pH 6.6 was unaltered (2.6 ± 0.3) compared with that at pH 7.4, whereas Cu^{2+}-precipitated Aβ1–42 bound ~1 extra Cu^{2+} (3.3 ± 0.1) at pH 6.6 compared with pH 7.4 (Table 3).

Maximal Cu^{2+}-induced precipitation of Aβ1–40 was observed at pH 6.6 (91 ± 6%) compared with pH 7.4 (56 ± 6%; Table 3 and Fig. 3B and D). In contrast, maximal Cu^{2+}-induced Aβ1–42 precipitation was similar at either pH (72 ± 10 and 65 ± 12% for pH 7.4 and 6.6, respectively; Table 3 and Fig. 3B and D). Maximally precipitated Aβ1–40 bound ~2.5 Cu^{2+} at both pH 7.4 and 6.6, even though precipitation was 35% greater at pH 6.6. Also, although maximal Cu^{2+}-induced Aβ1–42 precipitation was 17% greater than that of Aβ1–40 at pH 7.4, it was 26% less than that of Aβ1–40 at pH 6.6, even

TABLE 3. *Stoichiometry of Cu(II) binding to soluble (or minimal precipitated) and precipitated Aβ1–40 and Aβ1–42 at pH 7.4 and 6.6*

	Bound Cu(II):Aβ1–40		Bound Cu(II):Aβ1–42	
	Soluble/minimal precipitation	Maximal precipitation	Soluble/minimal precipitation	Maximal precipitation
pH 7.4	0.14 ± 0.10 (10.6)	2.35 ± 0.22 (1.8–6.6)	0.25 ± 0.18 (17.0)	2.59 ± 0.17 (1.8–6.6)
	[5.1 ± 3.9%] {5}	[55.7 ± 6.0%] {27}	[17.4 ± 8.2%] {6}	[72.4 ± 10.3%] {28}
pH 6.6	0.17 ± 0.20 (15.5)	2.55 ± 0.29 (1.0–5.8)	0.30 ± 0.10 (16.2)	3.25 ± 0.07 (1.0–5.8)
	[2.1 ± 1.7%] {5}	[91.1 ± 5.9%] {24}	[53.1 ± 14.9%] {6}	[64.9 ± 12.4%] {28}

Data for soluble/minimal precipitation are mean ± SD stoichiometry of metal:Aβ binding in the soluble fraction at the lowest log K_{app} of the competitor metal:chelator complex where Aβ remains either "soluble" (<10% precipitated for Aβ1–40) or least precipitated (for Aβ1–42) (log K_{app} = log K_{app} value of competing metal:chelator complex where minimal Aβ precipitation occurs) [average ± SD minimal percent Aβ precipitation] {n = no. of data points}. Data for maximal precipitation are average ± SD stoichiometry of metal:Aβ precipitate where peptide precipitation has plateaued at maximal for the series of competitor metal:chelator complexes (log K_{app} range = log K_{app} values of competing metal:chelator complexes where maximal Aβ precipitation occurs) [average ± SD maximal percent Aβ precipitation] {n = no. of data points}.

TABLE 4. *Competition between Cu^{2+} and Zn^{2+} for metal ion binding sites on Aβ1–40 at pH 7.4 and 6.6*

	pH 7.4	pH 6.6
Zn^{2+} + Aβ, 48 h		
% precipitation	88.4 ± 0.9	85.0 ± 0.4[a]
Ratio Zn:Aβ	2.88 ± 0.03	2.03 ± 0.19[a]
Cu^{2+} + Aβ, 48 h		
% precipitation	58.0 ± 3.9	85.4 ± 6.0[a]
Ratio Cu:Aβ	1.91 ± 0.15	2.76 ± 0.10[a]
Zn^{2+} + Cu^{2+} coincubated for 48 h		
% precipitation	79.0 ± 3.8	64.0 ± 7.2[b]
Ratio Zn:Aβ	1.90 ± 0.18	0.33 ± 0.09[a]
Ratio Cu:Aβ	1.68 ± 0.09	3.13 ± 0.05[a]
Total metal:Aβ ratio	3.58	3.46
Zn^{2+} for 24 h, then Cu^{2+} for 24 h		
% precipitation	65.8 ± 7.2	82.0 ± 4.1[a]
Ratio Zn:Aβ	1.74 ± 0.29	0.67 ± 0.22[a]
Ratio Cu:Aβ	1.48 ± 0.09	2.75 ± 0.04[a]
Total metal:Aβ ratio	3.22	3.22

The following incubations were done: (a) Aβ1–40 was incubated with 50 μ*M* Zn^{2+} for 48 h; (b) Aβ1–40 was incubated with 50 μ*M* Cu^{2+} for 48 h; (c) Aβ1–40 was incubated with 50 μ*M* Zn^{2+} and 50 μ*M* Cu^{2+} for 48 h; or (d) Aβ1–40 was incubated with 50 μ*M* Zn^{2+} for 24 h, 50 μ*M* Cu^{2+} was added, and the mixture was incubated for a further 24 h. Stoichiometry represents metal ion binding to total (precipitated and soluble) Aβ1–40. All experiments were done in Tris-buffered saline. Data are mean ± SD values (n = 6).

The statistical significance of comparisons between pH 7.4 and 6.6 for percent precipitation and ratio of metal:Aβ for each experiment was determined by *t* test (two-tailed, heteroscedastic): [a]$p < 0.001$, [b]$p < 0.005$.

though the aggregated Aβ1–42 bound 0.7 more Cu^{2+} at pH 6.6 than at pH 7.4.

Cu^{2+} initiates the nucleated precipitation of Aβ1–40 and Aβ1–42

Because, unlike Aβ1–40, the precipitation of Aβ1–42 did not correlate with the stoichiometry of bound Cu^{2+}, we studied the possibility that the precipitation of Aβ1–42 was by a seeding mechanism (Jarrett et al., 1993) where Cu^{2+} initiates peptide nucleation but that the precipitation of the majority of the solution was not metal-dependent. First, we measured the amount of precipitation of Aβ in the absence of added metal ions or chelators, incubated for 24 h under the same conditions as Fig. 3 and Table 3. The precipitation of Aβ1–40 and Aβ1–42 formed by an apparent seeding mechanism in the absence of metal ions or chelators was greater at pH 6.6 (23 ± 7 and 95 ± 4%, respectively) than at pH 7.4 (10 ± 2 and 87 ± 1%), in agreement with our previous report (Atwood et al., 1998). It is surprising that the precipitation of Aβ1–40 or Aβ1–42 at pH 6.6 in the absence of added metal ions was greater than the corresponding amount of Aβ1–40 or Aβ1–42 precipitation that occurred in the presence of 50 μ*M* Cu^{2+} that had been complexed with any of the high-affinity chelators (log $K_{app} \geq 10.6$; Fig. 3B and D). To illustrate this, in Fig. 5A we compare the precipitation of Aβ1–40 and Aβ1–42 in the presence and absence of the DPTA:Cu^{2+} complex. We studied DTPA because NMR spectroscopy of DTPA coincubated with Aβ1–40 and Aβ1–42 indicated that the chelator does not bind to the peptide (X. Huang, K. Barnham, C. S. Atwood, R. E. Tanzi, and A. I. Bush, unpublished data); hence, any effect of DTPA in preventing Aβ precipitation is not due to β-sheet chain breaking. We observed that there is more precipitation of either Aβ1–40 or Aβ1–42 in the absence of added metal ions than in the presence of DPTA:Cu^{2+} complexes, at either pH (Fig. 5A). This indicates that the increased precipitation of Aβ at pH 6.6 in the absence of added metal ions could not be explained by pH effects alone and suggests that trace metal ion contamination of the buffers mediates the apparent seeding of Aβ solutions. Supporting this possibility, we measured the contaminating concentration of Cu^{2+} in buffer solutions containing Aβ as ~0.1 μ*M*, using inductive coupled plasma mass spectrometry.

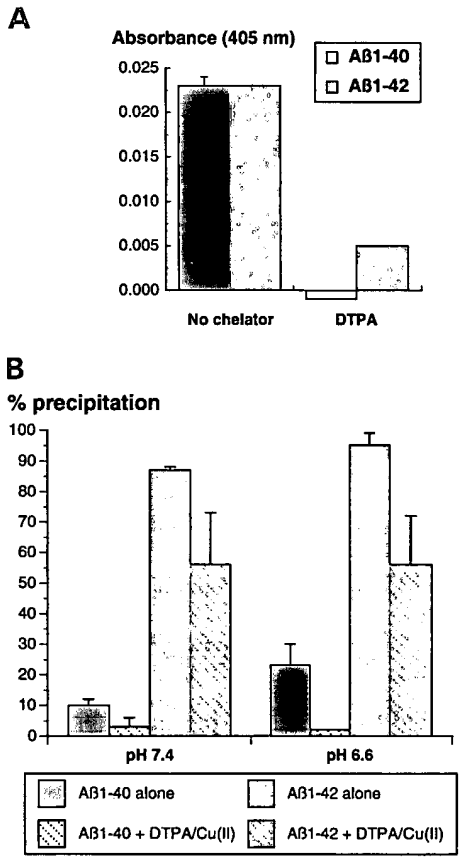

FIG. 5. Inhibition of Aβ nucleated precipitation by DTPA. **A:** Aβ1–40 or Aβ1–42 (10 μ*M*) was incubated at pH 7.4 and 6.6 with or without Cu^{2+}:DTPA complex (chelator complex data selected from Fig. 3B and D) for 24 h, and precipitation was determined as in Fig. 3. Data are mean ± SD (bars) values (n = 6). **B:** Aβ1–40 or Aβ1–42 (10 μ*M* each) was incubated in phosphate-buffered saline (pH 7.4) with or without DTPA (200 μ*M*) for 5 days at 37°C. Precipitation was assessed by measuring the turbidity of the solution at 405 nm. Data are mean ± SD (bars) values (n = 4).

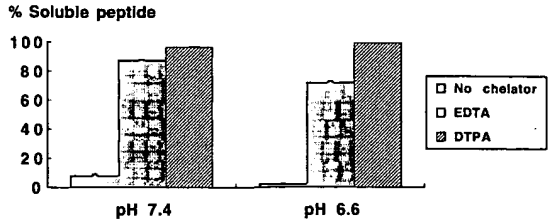

FIG. 6. Resolubilization of Cu–Aβ1–42 aggregates. Aβ1–42 (5 μ*M*) was precipitated by incubation in Tris-buffered saline with Cu^{2+} (20 μ*M*) for 1 h (37°C). Chelators (200 μ*M*; EDTA and DTPA) were then added to the reaction mixture for 1 h, the samples were centrifuged, and the supernatant was assayed for protein to determine the solubility of Aβ1–42. Data are mean ± SD (bars) values (n = 4).

To test if contaminating metal ions are necessary for the Aβ precipitation we had observed, we incubated Aβ solutions (10 μ*M*) in the presence or absence of DTPA (200 μ*M*) for 5 days. DTPA completely inhibited Aβ1–40 precipitation and markedly inhibited Aβ1–42 precipitation (Fig. 5B). Therefore, the increase in nucleation-driven peptide precipitation that was observed by lowering the pH of Aβ solutions from 7.4 to 6.6 in the absence of added metal (Fig. 5A) appears to be initiated by the precipitation of Aβ induced by the trace Cu^{2+} present, whose effects on Aβ are potentiated by the mildly acidic (pH 6.6) conditions (Atwood et al., 1998).

Reversibility of Cu^{2+}–Aβ aggregates by chelators

To determine whether chelators could resolubilize Aβ1–42 precipitated by Cu^{2+}, we preincubated Aβ1–42 (5 μ*M*) with Cu^{2+} (20 μ*M*) for 1 h before adding either no chelator or an excess of chelators of Cu^{2+} (EDTA or DTPA, 200 μ*M*; Fig. 6). In the absence of chelator, Cu^{2+} induced almost complete precipitation of Aβ1–42. However, both EDTA and DTPA effectively resolubilized (>88%) Cu–Aβ1–42 aggregates at pH 7.4. Under mildly acidic conditions (pH 6.6), the resolubilization of Cu–Aβ aggregates by EDTA and DTPA was 75 and 100% effective, respectively. Taken together, these data show that, like Aβ1–40 (Atwood et al., 1998), Aβ1–42 precipitation by Cu^{2+} is totally reversible through chelation.

pH-dependent competition between Cu^{2+} and Zn^{2+} for Aβ binding

To examine the ability of Cu^{2+} and Zn^{2+} to compete for metal ion binding sites on Aβ, we incubated Aβ1–40 with a mixture of Zn^{2+} and Cu^{2+} (50 μ*M* each) for 48 h at both pH 7.4 and 6.6. At pH 7.4, Zn^{2+} (1.9 ± 0.2) and Cu^{2+} (1.7 ± 0.1) simultaneously bound Aβ1–40 with approximately equal stoichiometry (Table 4). When this coincubation reaction was performed at pH 6.6, far more Cu^{2+} bound Aβ1–40 (3.1 ± 0.1) than Zn^{2+} (0.3 ± 0.1). Incubation of either Zn^{2+} or Cu^{2+} alone at pH 7.4 and 6.6 with Aβ1–40 for 48 h resulted in similar precipitation and stoichiometry as previously determined for a 24-h incubation (Fig. 3 and Table 4).

To determine whether Cu^{2+} could displace Zn^{2+} from binding sites in Zn–Aβ aggregates, we first preaggregated Aβ1–40 with Zn^{2+} (24-h incubation at pH 7.4 and 6.6 resulted in 88 ± 1 and 85 ± 0% precipitation, respectively) and then added an equimolar concentration of Cu^{2+} (50 μ*M*) to the reaction mixture for a further 24 h (Table 4). Determination of metal ion binding indicated 1.7 ± 0.3 Zn^{2+} ions and 1.5 ± 0.1 Cu^{2+} ions bound simultaneously to Aβ1–40 at pH 7.4. However, at pH 6.6 Cu^{2+} competed ~80% of the Zn^{2+} from binding sites on Aβ at pH 6.6 (0.5 Zn^{2+} and 2.8 Cu^{2+}). Therefore, Cu^{2+} displaced Zn^{2+} from Aβ1–40 only when the pH fell below neutrality. The decreased Zn^{2+} binding at pH 6.6 (Table 4) and the formation of new pH-dependent binding sites for Cu^{2+} may contribute to this effect.

Copper induces the formation of SDS-resistant polymers of Aβ

Recently, we have reported that Aβ reduces Cu^{2+} to Cu^{+} with the consequent generation of H_2O_2 (Huang et al., 1999). These reactions may contribute to the oxidative damage of Aβ that is reflected in SDS resistance of Alzheimer's amyloid (Masters et al., 1985; Roher et al., 1996). To determine whether Cu^{2+} could induce modifications of Aβ as reflected by changes in migration on SDS-PAGE, we incubated Aβ1–40 or Aβ1–42 with Cu^{2+}:Gly (30 μ*M*) for 1 day (Fig. 7). Cu^{2+} induced the formation of higher-molecular-weight species of both Aβ1–40 and Aβ1–42 on SDS-PAGE (Fig. 7). Aβ1–40 exhibited a 5.2 and ≤1% increase in apparent dimeric and trimeric species of relative molecular mass of ~8.6 and 13 kDa, respectively, after a 1-day incubation. Aβ1–42 was more sensitive to Cu^{2+}-induced modification, with 31.1 and 12.5% of the peptide identified as apparent 13- and ≥17-kDa species after a 1-day incubation. In contrast to Aβ1–40, ≤1% of Aβ1–42 incubated with Cu^{2+} was detectable as the 8.6-kDa species. Therefore, although Cu^{2+}-induced precipitation of Aβ is reversible using chelation after a 1-h incubation (Fig. 6), prolonged coincubation with Cu^{2+} (24 h) generates some SDS-resistant forms.

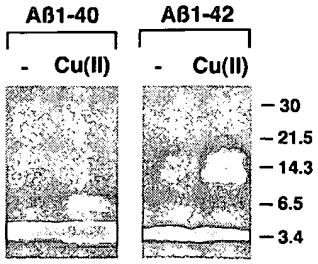

FIG. 7. Copper-induced apparent oligomerization of human Aβ. Aβ (2.5 μ*M*) was brought to 150 m*M* NaCl and 66 m*M* phosphate (pH 7.4) with or without Cu^{2+} (30 μ*M*). Samples were incubated at 37°C for 1 day, and aliquots were analyzed by western blotting (6E10 antibody). Molecular size markers are shown. Similar results were obtained using monoclonal antibody 4G8.

DISCUSSION

CMCA

The CMCA technique was developed for the practical assessment of stoichiometry and affinities of metal ion binding to soluble and precipitated proteins. Validation of our methodology was obtained by a comparison of Cu^{2+} and Zn^{2+} binding affinities with the known affinities for DSA (Fig. 2). This technique circumvents several problems associated with preexisting methodologies for the assessment of metal ion binding to proteins. Competition studies often require the use of expensive and hazardous radioactive metal ions or ligands, and spectrophotometric or fluorescence techniques lack sensitivity in the submicromolar metal ion concentration range and rely on conformational changes in the target protein.

Despite these advantages, the CMCA method relies on the availability of an array of chelators that reflect log K_{app} values within the range of interest. To this end, we attempted to provide chelators at log K_{app} intervals of no more than 0.5 units, but the number of usable chelators with log $K_{app} > 10$ was small. The array of data points required by this technique should be improved as we identify further appropriate chelators for use in the assay.

Binding interactions with Cu^{2+} differentiate Aβ1–40 and Aβ1–42

Our current results, summarized in Table 2, indicated multiple affinity Cu^{2+} binding sites on Aβ1–40 and Aβ1–42 that were considerably greater than the single affinities (4.0 and 0.3 μM, respectively) initially obtained for the peptides using spectrophotometric analysis (Atwood et al., 1998). This apparent discrepancy is probably because, in the previous study, the precipitation of the peptide by Cu^{2+} withdrew a fraction of the peptide from spectral analysis and may have artifactually lowered the sensitivity of the technique to detect physicochemical changes. Also, the spectrometric analysis we used previously would have been only capable of appreciating spectral shifts associated with saturation of the lower-affinity Cu^{2+} binding site on Aβ. This is because in our previous analysis we measured the spectroscopic response of synthetic peptide to increments of ≥ 0.1 μM in Cu^{2+} concentration. Because the background contamination of the incubation buffer with Cu^{2+} is ~ 0.1 μM and because we have now identified Cu^{2+} binding sites on Aβ with subnanomolar affinities, the previous technique could not have reliably titrated the Cu^{2+} concentration in low nanomolar increments to appreciate a consequent spectroscopic effect. An advantage of the current CMCA technique was that we could titrate the physicochemical effects of the exchange of Cu^{2+} to Aβ against the known binding affinities of chelators in competition for Cu^{2+}, without the need to titrate metal ion concentrations that are below background contamination levels.

The estimated log K_{app} for the Cu^{2+} binding site on Aβ1–42 (log K_{app} = 17.2; Table 2) translates into a predicted affinity for Cu^{2+} in the attomolar range and for Aβ1–40 in the picomolar range (estimated log K_{app} = 10.3; Table 2), indicating that Cu^{2+} could be bound to Aβ (Aβ1–42 ≫ Aβ1–40) under biological conditions. Also, the concave acceleration of the Scatchard analyses of Cu^{2+} binding to Aβ1–40 and Aβ1–42 (Fig. 3E) suggests negative cooperativity of the binding sites. Aβ1–42 was found to have significantly less hindrance in binding successive Cu^{2+} ions compared with Aβ1–40. Aβ1–42 also exhibits higher affinity Cu^{2+} binding than Aβ1–40 at both the lowest- and highest-affinity binding sites observed, which indicates that the structural basis for Cu^{2+} binding and the allosteric basis for cooperativity may be mediated by the hydrophobic carboxyl-terminal tail of Aβ. Aβ1–42 reportedly has a higher β-sheet content than Aβ1–40 (Barrow et al., 1992), and β-sheet or β-barrel conformations are known to mediate other high-affinity Cu binding sites (Fraústo da Silva and Williams, 1993). The increased β-sheet content of Aβ1–42 makes the peptide more liable to self-associate and to precipitate (Jarrett et al., 1993). This self-association could have an allosteric impact on Cu^{2+} binding, especially if Cu^{2+} binding to Aβ involves multmeric interactions between protein subunits, It is also possible that nucleated precipitation of Aβ1–42 (see below) may have perturbed the equilibrium of bound to free soluble Cu^{2+} as the Cu^{2+} is removed from the soluble phase, thus contributing to the log K_{app} value we have observed. However, the possibility of irreversible withdrawal of Cu^{2+} associated with the precipitating peptide was not supported by our observation that high-affinity Cu chelators resolubilized Cu^{2+}-associated Aβ1–42 deposits (Fig. 6). It is also unlikely that our results only reflect Cu^{2+} binding to preassociated Aβ because the precipitation of soluble Aβ in the presence of Cu^{2+} occurs within seconds (Atwood et al., 1998) but over days in the absence of added metal ions (Jarrett et al., 1993). Nevertheless, preliminary data indicate Cu^{2+} binds to fibrillized Aβ with approximately the same stoichiometry as to fresh soluble Aβ (C. S. Atwood et al., unpublished data).

The structures of the multiple Cu^{2+} binding sites on soluble and precipitated Aβ are not yet clear and could be complex because new sites may form during the assembly of the peptide. Some evidence suggests that Aβ forms a dimer in solution (Garzon-Rodriguez et al., 1997; Huang et al., 1997). Therefore, the noninteger stoichiometry of 0.5 equivalents that was clearly observed for the highest-affinity binding site on Aβ1–42 and 2.5 equivalents for the lowest-affinity Cu^{2+} binding site on both Aβ1–40 and Aβ1–42 at pH 6.6 (Fig. 3E and Table 2) may reflect interaction with Aβ dimers. It is also possible that some binding sites are created by residues on neighboring Aβ subunits that are only brought into Cu^{2+}-coordinating alignment as the peptide aggregates.

We have also shown for the first time that Cu^{2+} slowly modifies Aβ, inducing SDS resistance (Fig. 7). Previous studies have shown that Fe/H_2O_2 oxidation systems promote SDS-resistant polymerization of Aβ generated in a wheat germ expression system (Dyrks et al., 1992), but

we found that Cu^{2+} promotes the polymerization of both synthetic Aβ1–40 and Aβ1–42 in the absence of added H_2O_2 (Fig. 7). Our recently reported findings that the Aβ peptide directly produces H_2O_2 through Cu^{2+} reduction (Huang et al., 1999*a*,*b*) may contribute to the slow oxidation of the peptide.

The linear relationship between Cu^{2+} binding stoichiometry to Aβ1–40 and peptide precipitation (from zero in the soluble state to 2–3 in the precipitated state) was maintained at both pH 6.6 and 7.4 (Figs. 3 and 4), indicating that the increase in Cu^{2+} binding stoichiometry to Aβ1–40 at pH 6.6 that we observed (Figs. 3 and 4 and Table 3) probably reflects saturation of Cu^{2+} binding sites (at $\approx$2.5 equivalents) coordinated by Aβ rather than the creation of new binding sites. There was a similar increase in Cu^{2+} binding stoichiometry to Aβ1–42 at pH 6.6, but this did not correlate with increased precipitation, probably because the seeding mechanism of precipitation (Jarrett et al., 1993; discussed below) influenced Aβ1–42 far more than Aβ1–40. Aβ1–42 was observed to be soluble only when it bound no Cu^{2+} (Fig. 3A and B and Table 3).

Cu^{2+}-mediated peptide assemblies nucleate Aβ1–42 precipitation

Precipitation of Aβ also occurred in the absence of added metal ions, but we attribute this to interaction of the peptide with trace metal ion contamination in the buffers that is difficult to remove without chelation (Figs. 5 and 6). Our evidence suggests that trace amounts of metal ions are sufficient to induce Aβ nucleation, which causes the remainder of the Aβ solution to precipitate by a seeding mechanism (Jarrett et al., 1993). We have found that concentrations of Cu and other metal ions are commonly ~0.1 μM each in our laboratory buffer systems, even those treated with chelating resins such as Chelex-100. It is very difficult to prevent trace contamination with metal ions because the metals dissolve from solutions contacting air (Huang et al., 1994). Mildly acidic conditions (pH 6.6) increased the precipitation of Aβ in the absence of added metal ions (Fig. 5), which is typical of the enhancement of Aβ precipitation induced by Cu^{2+}- and Fe^{3+} but not Zn^{2+} (Atwood et al., 1998), and also was abolished by DTPA, a high-affinity Cu^{2+}-selective chelator that does not bind to the peptide. The possibility that Fe^{3+} may be another trace metal ion contaminating the buffer system and contributing to acidity-enhanced Aβ precipitation cannot yet be excluded, but Fe^{3+} induces far less precipitation of Aβ than Cu^{2+} under similar conditions (Atwood et al., 1998). We had previously shown that the precipitation of Aβ1–40 by Zn^{2+} (Huang et al., 1997) or Cu^{2+} (Atwood et al., 1998) could be reversed in the presence of a chelator. Our results now indicate that metal ion-induced precipitation of Aβ1–42 also is reversible in the presence of high-affinity metal ion chelators (Fig. 6). Most important is that we now report for the first time that the spontaneous Aβ1–42 aggregation that occurs with "aging" the peptide over days in aqueous solution (Jarrett et al., 1993) also can be prevented by the presence of the high-affinity copper-selective chelators. These data indicate that trace metal ion contamination is likely to be a major factor in the incubation-dependent Aβ aggregation process.

Nucleation-mediated precipitation appears to have contributed far more to the Cu^{2+}-mediated precipitation of Aβ1–42 we observed than to the Cu^{2+}-mediated precipitation of Aβ1–40 (Figs. 3 and 5). Although there was a strict correspondence between the stoichiometry of bound Cu^{2+} and the amount of Aβ1–40 precipitation (R^2 = 0.89 at pH 7.4 and 0.85 at pH 6.6; Fig. 4), there was a weak correlation (and at pH 6.6, no correlation) between the stoichiometry of bound Cu^{2+} and the amount of Aβ1–42 precipitation (R^2 = 0.17 at pH 7.4 and 0.09 at pH 6.6; Fig. 4). This may be because Aβ1–42 is much more sensitive to nucleation-mediated precipitation than Aβ1–40 (Jarrett et al., 1993). Therefore, even a trace amount of nucleated Aβ formed by interaction with Cu^{2+} initiates near-complete precipitation of the Aβ1–42 solution (Figs. 3 and 5B). Our data also indicate how difficult it is to prevent Cu^{2+}-induced nucleation in a solution of Aβ1–42, requiring the use of chelators with very high affinity for Cu^{2+} (Fig. 3B).

Mildly acidic conditions promote the binding of Cu^{2+} but not Zn^{2+} to Aβ

The mechanism for enhanced Cu^{2+} binding to Aβ1–40 and Aβ1–42 at pH 6.6 compared with pH 7.4 is still unclear. It may involve [H^+]-induced conformational changes in the peptide because previous evidence indicates that soluble Aβ is mainly α-helical at pH >7 but mainly β-sheet between pH 4 and 7 (Soto et al., 1994). The increased β-sheet content expected at pH 6.6 may promote access of Cu^{2+} to the metal binding sites on Aβ, exposing a low-affinity Cu^{2+} binding site that is not accessible at pH 7.4.

We have previously shown that Cu^{2+}-induced precipitation of Aβ under mildly acidic conditions (pH 6.6) is mediated, at least partly, by the coordination of Cu^{2+} via His residues (Atwood et al., 1998). Whereas acidic conditions will lead to the protonation of amino acids with side chains containing an ionizable group, e.g., His or Lys, the pK_a of the His side chain in Aβ1–40 is ~6.5 (Coles et al., 1998), indicating that a significant proportion of imidazole residues is still unprotonated under our pH conditions (pH 7.4 and 6.6). The effect of lowering pH from 7.4 to 6.6 in promoting selective Cu^{2+} binding in the presence of Zn^{2+} (Table 4) may relate to the lower proportion of unprotonated His side chains available for metal coordination, decreasing from ~90% (pH 7.4) to 50% (pH 6.6) over this pH range. This would, however, require Zn^{2+} to be more sensitive than Cu^{2+} to the availability of multiple His residues. Alternatively, if there was a carboxylate Zn^{2+}-ligand buried in a sheet and with an unusually high pK_a of near 6–7 (instead of the normal 5) that was undergoing protonation in this pH range, this could also account for reduced Zn^{2+} binding at pH 6.6. Another possibility is that an amide nitrogen

deprotonates and selectively coordinates to Cu^{2+}. Our recent electron paramagnetic resonance evidence has indicated a coordination sphere for Cu^{2+} to Aβ of CuN_3O_1 (Huang et al., 1999*b*), and detailed simulations reveal that only two of these nitrogens are His residues, whereas the third is a deprotonated amide-N. When Cu^{2+} coordinates to an amide nitrogen, it is able to increase dramatically the acidity of the amide NH to <7 and as low as 4, whereas the pK_a of amides bound to Zn^{2+} is still ~12 (Sigel and Martin, 1982). This selective stabilization of a deprotonated (anionic) amide is the result of more effective ligand-to-metal charge transfer from the deprotonated amide nitrogen to the d^9 Cu^{2+} versus a d^{10} Zn^{2+} transition metal ion. This is a common phenomenon among other electrophilic transition metal ions with vacant *d* orbitals (Woon and Fairlie, 1992). Therefore, we propose that although His residues may contribute to the coordination of both Cu^{2+} and Zn^{2+} sites, one amide group may coordinate an additional low-affinity Cu^{2+} as the pH is lowered from 7.4 to 6.6, whereas high-affinity Cu^{2+} coordination and Zn^{2+} coordination may be simultaneously weakened. A similar increase in Cu^{2+} binding in response to acidic pH (pH 3–6) has recently been reported for the multicopper oxidase apoFet3p (Davis-Kaplan et al., 1998).

Possible physiological and pathological roles for the selective Cu^{2+} and Zn^{2+} binding sites on Aβ

Our data indicate that Aβ binds approximately equivalent amounts of Cu^{2+} and Zn^{2+} at pH 7.4 but that Cu^{2+} totally displaces Zn^{2+} binding to Aβ at pH 6.6. We have previously published the finding that at pH 7.4 the Zn^{2+} binding site is very highly selective for Zn^{2+} and that at pH 7.4 Zn^{2+} cannot be displaced from binding Aβ by overwhelming concentrations of Cu^{2+} or any other transition metal ion (Bush et al., 1994*a*). Taken together with our current results, we hypothesize that Aβ possesses highly selective Cu^{2+} and Zn^{2+} binding sites at pH 7.4 but that at pH 6.6 there is a weakened affinity for Zn^{2+} but a preserved affinity for Cu^{2+} that allows the peptide to become occupied by Cu^{2+} at both sites. Thus, excessive Cu^{2+} binding of Aβ may be a consequence of mild acidosis and may have a deleterious promoting effect on the aggregation and the redox activities (Huang et al., 1999*a*,*b*; present study, Fig. 7) of the protein.

Low-affinity metal binding sites on Aβ mediate aggregation and precipitation and also may mediate Cu^{2+} reduction, O_2-dependent H_2O_2 production (Huang et al., 1999*a*), and oxidative modification of Aβ (Fig. 7). It is possible that one of the low-affinity Cu^{2+} sites we have observed may be due to Cu^{2+} occupying the Zn^{2+} site on Aβ. Abnormal Cu^{2+} binding to the Zn^{2+} binding site on wild-type and mutant superoxide dismutase has been shown to alter the redox chemistry of this protein and to promote radical generation, which may play a pathogenic role in familial amyotrophic lateral sclerosis (Goto et al., 1998). We contemplate similarities between this abnormal neurochemistry in familial amyotrophic lateral sclerosis and abnormal Aβ–metal interactions in AD.

Abnormal Cu/Zn interactions with Aβ in AD

Zn and Cu ions mediate the precipitation of Aβ deposits in AD brain as evidenced by the solubilization of Aβ from postmortem AD brain tissue that is promoted by chelators selective for these metals (Cherny et al., 1999) and also evidenced by the marked enrichment of total Cu and Zn in AD neuropil and amyloid plaques (Lovell et al., 1998), which could be explained by the high affinity of these metal ions for Aβ (present study, Fig. 3 and Table 2; Bush et al., 1994*a*; Atwood et al., 1998). It is not yet clear whether abnormal Cu (or Zn) homeostasis initiates Aβ deposition, or whether the accumulation of Aβ acts as a sink that draws metal ions into its mass. Significant increases in the concentration of Cu in the CSF [2.2-fold (Basun et al., 1991)] accompanied by an increase in level of CSF and brain ceruloplasmin, a Cu transport protein, in AD patients (Loeffler et al., 1994) further indicate that Cu homeostasis is compromised in AD.

Both Cu and Zn are released from vesicles of neurons during synaptic transmission reaching concentrations as high as 15 μ*M* (Hartter and Barnea, 1988) and 300 μ*M* (Frederickson, 1989), respectively. The proportion of binding of Cu and Zn to Aβ will depend on the respective stability constants of each metal ion for different ligands, their total concentrations, and the pH of the microenvironment. The release of Cu and Fe from metalloproteins is usually promoted by mildly acidic environments (reviewed by Atwood et al., 1998). However, under mildly acidic conditions Cu^{2+} binding to Aβ was enhanced, almost completely displacing Zn^{2+} from Aβ (Table 3). This unusual property of Aβ to accept Cu^{2+} under mildly acidic conditions, where most proteins lose metal ions with decreasing pH, may be important in the pathophysiology of AD, where metabolic compromise may result in acidosis (Yates et al., 1990).

Acknowledgment: The authors thank Diane Cabelli, Alan Kay, J. D. Robertson, and Kevin Barnham for helpful discussions. This work is supported by funds from the National Institutes of Health (grant R29AG12686), PRANA Corp., and the American Health Assistance Foundation.

REFERENCES

Appleton D. W. and Sarkar B. (1971) The absence of specific copper (II)-binding site in dog albumin. *J. Biol. Chem.* **246**, 5040–5046.

Atwood C. S., Moir R. D., Huang X., Bacarra N. M. E., Scarpa R. C., Romano D. M., Hartshorn M. A., Tanzi R. E., and Bush A. I. (1998) Dramatic aggregation of Alzheimer Abeta by Cu(II) is induced by conditions representing physiological acidosis. *J. Biol. Chem.* **273**, 12817–12826.

Barrow C. J., Yasuda A., Kenny P. T., and Zagorski M. G. (1992) Solution conformations and aggregational properties of synthetic amyloid beta-peptides of Alzheimer's disease. Analysis of circular dichroism spectra. *J. Mol. Biol.* **225**, 1075–1093.

Basun H., Forssell L. G., Wetterberg L., and Winblad B. (1991) Metals and trace elements in plasma and cerebrospinal fluid in normal

aging and Alzheimer's disease. *J. Neural Transm. Park. Dis. Dement. Sect.* **3,** 231–258.

Bush A. I., Pettingell W. H. Jr., Paradis M. D., and Tanzi R. E. (1994*a*) Modulation of Aβ adhesiveness and secretase site cleavage by zinc. *J. Biol. Chem.* **269,** 12152–12158.

Bush A. I., Pettingell W. H., Multhaup G., Paradis M. D., Vonsattel J. P., Gusella J. F., Beyreuther K., Masters C. L., and Tanzi R. E. (1994*b*) Rapid induction of Alzheimer A beta amyloid formation by zinc. *Science* **265,** 1464–1467.

Bush A. I., Moir R. D., Rosenkranz K. M., and Tanzi R. E. (1995) Zinc and Alzheimer's disease—response. *Science* **268,** 1921–1923.

Cherny R. A., Legg J. T., McLean C. A., Fairlie D. P., Huang X., Atwood C. S., Beyreuther K., Tanzi R. E., Masters C. L., and Bush A. I. (1999) Aqueous dissolution of Alzheimer's disease Aβ amyloid deposits by biometal depletion. *J. Biol. Chem.* **274,** 23223–23228.

Clements A., Allsop D., Walsh D. M., and Williams C. H. (1996) Aggregation and metal-binding properties of mutant forms of the amyloid Aβ peptide of Alzheimer's disease. *J. Neurochem.* **66,** 740–747.

Coles M., Bicknell W., Watson A. A., Fairlie D. P., and Craik D. J. (1998) Solution structure of amyloid beta-peptide(1–40) in a water-micelle environment. Is the membrane-spanning domain where we think it is? *Biochemistry* **37,** 11064–11077.

Cornett C. R., Markesbery W. R., and Ehmann W. D. (1998) Imbalances of trace elements related to oxidative damage in Alzheimer's disease brain. *Neurotoxicology* **19,** 339–345.

Davis-Kaplan S. R., Askwith C. C., Bengtzen A. C., Radisky D., and Kaplan J. (1998) Chloride is an allosteric effector of copper assembly for the yeast multicopper oxidase Fet3p: an unexpected role for intracellular chloride channels. *Proc. Natl. Acad. Sci. USA* **95,** 13641–13645.

Dawson R. M. C., Elliott D. C., Elliott W. H., and Jones K. M. (1986) *Data for Biochemical Research,* 3rd edit., pp. 399–415. Oxford University Press, Oxford.

Deibel M. A., Ehmann W. D., and Markesbery W. R. (1996) Copper, iron, and zinc imbalances in severely degenerated brain regions in Alzheimer's disease: possible relation to oxidative stress. *J. Neurol. Sci.* **143,** 137–142.

Dyrks T., Dyrks E., Hartmann T., Masters C., and Beyreuther K. (1992) Amyloidogenicity of beta A4 and beta A4-bearing amyloid protein precursor fragments by metal-catalyzed oxidation. *J. Biol. Chem.* **267,** 18210–18217.

Ehmann W. D., Markesbery W. R., Alauddin M., Hossain T. I., and Brubaker E. H. (1986) Brain trace elements in Alzheimer's disease. *Neurotoxicology* **7,** 195–206.

Fraústo da Silva J. J. R. and Williams R. J. P. (1993) *The Biological Chemistry of the Elements (The Inorganic Chemistry of Life).* Oxford University Press, Oxford.

Frederickson C. J. (1989) Neurobiology of zinc and zinc-containing neurons. *Int. Rev. Neurobiol.* **31,** 145–238.

Garzon-Rodriguez W., Sepulveda-Becerra M., Milton S., and Glabe C. G. (1997) Soluble amyloid Abeta-(1–40) exists as a stable dimer at low concentrations. *J. Biol. Chem.* **272,** 21037–21044.

González C., Martin T., Cacho J., Brañas M. T., Arroyo T., Garcia-Berrocal B., Navajo J. A., and González-Buitrago J. M. (1999) Serum zinc, copper, insulin and lipids in Alzheimer's disease epsilon 4 apolipoprotein E allele carriers. *Eur. J. Clin. Invest.* **29,** 637–642.

Goto J. J., Gralla E. B., Valentine J. S., and Cabelli D. E. (1998) Reactions of hydrogen peroxide with familial amyotrophic lateral sclerosis mutant human copper–zinc superoxide dismutase studied by pulse radiolysis. *J. Biol. Chem.* **273,** 30104–30109.

Goumakos W., Laussac J.-P., and Sarkar B. (1971) Binding of cadmium(II) and zinc(II) to human and dog serum albumins. An equilibrium dialysis and ^{113}Cd-NMR study. *Biochem. Cell Biol.* **69,** 809–820.

Gray D. N., Cherny R. A., Masters C. L., Tanzi R. E., and Bush A. I. (1998) Resolubilization of Alzheimer and APP transgenic beta amyloid plaque by copper chelators. *Soc. Neurosci. Abstr.* **24,** 722.

Hartter D. E. and Barnea A. (1988) Evidence for release of copper in the brain: depolarization-induced release of newly taken-up ^{67}copper. *Synapse* **2,** 412–415.

Hershey C. O., Hershey L. A., Varnes A., Vibhakar S. D., Lavin P., and Strain W. H. (1983) Cerebrospinal fluid trace element content in dementia: clinical, radiologic, and pathologic correlations. *Neurology* **33,** 1350–1353.

Huang X., Olmez I., and Aras N. K. (1994) Emissions of trace elements from motor vehicles: potential marker elements and source composition profile. *Atmospheric Environ.* **28,** 1385–1391.

Huang X., Atwood C. S., Moir R. D., Hartshorn M. A., Vonsattel J.-P., Tanzi R. E., and Bush A. I. (1997) Zinc-induced Alzheimer's Aβ1–40 aggregation is mediated by conformational factors. *J. Biol. Chem.* **272,** 26464–26470.

Huang X., Cuajungco M. P., Atwood C. S., Hartshorn M. A., Tyndall J., Hanson G. R., Stokes K. C., Multhaup G., Goldstein L. E., Scarpa R. C., Saunders A. J., Lim J., Moir R. D., Glabe C., Bowden E. F., Masters C. L., Fairlie D. P., Tanzi R. E., and Bush A. I. (1999*a*) Cu(II) potentiation of Alzheimer Aβ neurotoxicity: correlation with cell-free hydrogen peroxide production and metal reduction. *J. Biol. Chem.* **274,** 37111–37116.

Huang X., Atwood C. S., Hartshorn M. A., Multhaup G., Goldstein L. E., Scarpa R. C., Cuajungco M. P., Gray D. N., Lim J., Moir R. D., Tanzi R. E., and Bush A. I. (1999*b*) The Aβ peptide of Alzheimer's disease directly produces hydrogen peroxide through metal ion reduction. *Biochemistry* **38,** 7609–7616.

Jarrett J. T., Berger E. P., and Lansbury P. T. Jr. (1993) The carboxy terminus of the beta amyloid protein is critical for the seeding of amyloid formation: implications for the pathogenesis of Alzheimer's disease. *Biochemistry* **32,** 4693–4697.

Loeffler D. A., DeMaggio A. J., Juneau P. L., Brickman C. M., Mashour G. A., Finkelman J. H., Pomara N., and LeWitt P. A. (1994) Ceruloplasmin is increased in cerebrospinal fluid in Alzheimer's disease but not Parkinson's disease. *Alzheimer Dis. Assoc. Disord.* **8,** 190–197.

Lovell M. A., Robertson J. D., Teesdale W. J., Campbell J. L., and Markesbery W. R. (1998) Copper, iron and zinc in Alzheimer's disease senile plaques. *J. Neurol. Sci.* **158,** 47–52.

Makino T. (1991) A sensitive, direct colorimetric assay of serum zinc using nitro-PAPS and microwell plates. *Clin. Chim. Acta* **197,** 209–220.

Masters C. L., Simms G., Weinman N. A., Multhaup G., McDonald B. L., and Beyreuther K. (1985) Amyloid plaque core protein in Alzheimer disease and Down syndrome. *Proc. Natl. Acad. Sci. USA* **82,** 4245–4249.

Masuoka J., Hegenauer J., Van Dyke B. R., and Saltman P. (1993) Intrinsic stoichiometric equilibrium constants for the binding of zinc(II) and copper(II) to the high affinity site of serum albumin. *J. Biol. Chem.* **268,** 21533–21537.

Matsuba Y. and Takahashi Y. (1970) Spectrophotometric determination of copper with *N,N,N′,N′*-tetraethylthiuram disulfide and an application of this method for studies on subcellular distribution of copper in rat brain. *Anal. Biochem.* **36,** 182–191.

Ringblom A. (1963) *Complexation in Analytical Chemistry.* Interscience, New York.

Roher A. E., Chaney M. O., Kuo Y. M., Webster S. D., Stine W. B., Haverkamp L. J., Woods A. S., Cotter R. J., Tuohy J. M., Krafft G. A., Bonnell B. S., and Emmerling M. R. (1996) Morphology and toxicity of Abeta-(1–42) dimer derived from neuritic and vascular amyloid deposits of Alzheimer's disease. *J. Biol. Chem.* **271,** 20631–20635.

Samudralwar D. L., Diprete C. C., Ni B. F., Ehmann W. D., and Markesbery W. R. (1995) Elemental imbalances in the olfactory pathway in Alzheimer's disease. *J. Neurol. Sci.* **130,** 139–145.

Schwarzenbach G. and Flaschka H. (1969) *Complexometric Titrations.* Meuthuen, New York.

Shoji M., Golde T. E., Ghiso J., Cheung T. T., Estus S., Shaffer L. M., Cai X.-D., McKay D. M., Tintner R., Frangione B., and Younkin S. G. (1992) Production of the Alzheimer amyloid beta protein by normal proteolytic processing. *Science* **258,** 126–129.

Sigel H. and Martin R. B. (1982) Coordinating properties of the amide bond. Stability and structure of metal ion complexes of peptides and related ligands. *Chem. Rev.* **82,** 385–459.

Soto C., Brañes M. C., Alvarez J., and Inestrosa N. C. (1994) Structural determinants of the Alzheimer's amyloid β-peptide. *J. Neurochem.* **63,** 1191–1198.

Spiro T. G. and Saltman P. (1969) *Structure and Bonding, Vol. 6.* Springer-Verlag, New York.

Suh S. W., Jensen K. B., Jensen M. S., Silva D. S., Kesslak J. P., Danscher G., and Frederickson C. J. (2000) Histological evidence implicating zinc in Alzheimer's disease. *Brain Res.* **852,** 274–278.

Thompson C. M., Markesbery W. R., Alaudin M., Hossain T. I. M., and Brubaker E. H. (1988) Regional brain trace-element studies in Alzheimer's disease. *Neurotoxicology* **9,** 1–8.

Vance D. E., Ehmann W. D., and Markesbery W. R. (1990) A search for longitudinal variations in trace element levels in nails of Alzheimer's disease patients. *Biol. Trace Element Res.* **26–27,** 461–470.

Vigo-Pelfrey C., Lee D., Keim P., Lieberburg I., and Schenk D. B. (1993) Characterization of β-amyloid peptide from human cerebrospinal fluid. *J. Neurochem.* **61,** 1965–1968.

Woon T. C. and Fairlie D. P. (1992) Amide complexes of diethylenetriamineplatinum(II). *Inorg. Chem.* **31,** 4069–4074.

Yates C. M., Butterworth J., Tennant M. C., and Gordon A. (1990) Enzyme activities in relation to pH and lactate in postmortem brain in Alzheimer-type and other dementia. *J. Neurochem.* **55,** 1624–1630.